On the Approximation Solution of a Cellular Automaton Traffic Flow Model and Its Relationship with Synchronized Flow

R. Jiang[1,2], Y.M. Yuan[1], and K. Nishinari[2]

[1] School of Engineering Science, University of Science and Technology of China,
Hefei 230026, China
[2] Department of Aeronautics and Astronautics, School of Engineering,
The University of Tokyo, Hongo, Bunkyo-ku, Tokyo 113-8656, Japan

Abstract. This paper studies approximation solution of a cellular automaton model. In the model, the finite size effect is trivial because the congested flow is quite homogeneous. Thus, the approximation solution of a small sized system can be regarded as solution of large system. We have investigated the approximation solution of a small traffic system with two vehicles. The analytical result is in good agreement with simulation. Finally, it is demonstrated that the homogeneous congested flow is closely related to synchronized flow.

Keywords: traffic flow, cellular automaton, synchronized flow.

1 Introduction

Recently, the vehicular traffic problem has attracted the interests of physicists [1-6]. On the one hand, the researches contribute to traffic planning, design, control and implementation of transportation network by revealing the basic principles governing traffic congestion. On the other hand, vehicular traffic, as a system of interacting particles driven far from equilibrium, offers the possibility to study various fundamental aspects of nonequilibrium systems.

To simulate the various traffic phenomena, many traffic flow models are proposed. These models could be generally classified into macroscopic continuum models, mesoscopic kinetic models, microscopic car-following models and cellular automaton (CA) models. We focus on CA models in this paper.

In 1992, Nagel and Schreckenberg proposed the well known NaSch model [7]. They extended the CA-184 rules, in which the maximum velocity $v_{max} = 1$, to case $v_{max} > 1$. Together with the randomization effect, the NaSch model could reproduce the spontaneous formation of jams in congested traffic. Since then, a large number of papers that improve NaSch models have been published. Analytical theories of the NaSch model are also developed (see Ref.[2] and references therein).

In recent years, Kerner and his colleagues found that congested flow can be further classified into synchronized flow and wide moving jams [1,8-12]. Different

from wide moving jams, which exhibit the characteristic to maintain a constant mean velocity of the downstream jam front, synchronized flow is usually fixed at bottlenecks. Empirical observations show that a two-dimensional scattering of empirical data on flow-density plane is identified in synchronized flow.

On an open road with an isolated on-ramp, it is found that when the on-ramp flow rate is high, the onset of congestion is usually associated with the transition from free flow to synchronized flow, and then moving jams emerge spontaneously in synchronized flow, usually at different location. However, widening synchronized flow pattern (WSP) could be observed when the on-ramp flow rate is low. No spontaneous jam occurs in WSP [1].

The NaSch model and the existing NaSch-based models fail to reproduce the synchronized flow, because randomization effect always triggers avalanche-like braking of vehicles and finally leads to jams in congested flow.

In this paper, we present a simple CA model, in which homogeneous congested flow is reproduced. It is demonstrated that the homogeneous congested flow is closely related to synchronized flow. Furthermore, we present an approximation solution of the model. This is achieved because the finite size effect is trivial in the model.

The paper is organized as follows. In section II, the model is introduced. Section III presents the approximation solution of the model. Section IV discusses the relationship between homogeneous congested flow and synchronized flow. The conclusion is given in Section V.

2   Model

In this paper, we present a simple CA model, the approximation solution of which could be obtained. The parallel update rules of our model are as follows.

- Velocity adjustment:
  $$v_n(t+1) = \min(v_n(t) + 1, v_{\max}, d_n(t), v'),$$
  where $v' = \left\lfloor \dfrac{-T + \sqrt{T^2 + \frac{2}{D}\left(d_n(t) + \frac{v_{n-1}^2(t)}{2D}\right)}}{1/D} \right\rfloor$

- Randomization:
  $$v_n(t+1) = \max(v_n(t+1) - 1, 0) \text{ with probability } p_d$$

- Movement:
  $$x_n(t+1) = x_n(t) + v_n(t+1)$$

Here $v_{\max}$ is maximum velocity, D is a comfortable deceleration, T is reaction time, $\lfloor x \rfloor$ is the maximum integer that is not larger than x, $d_n = x_{n-1} - x_n - l$ is spatial gap in front of vehicle n, l is vehicle length.

The only difference between our model and NaSch model is introduction of v', which is obtained from

$$\frac{v'^2}{2D} + v'T = \frac{v_{n-1}^2(t)}{2D} + d_n(t). \tag{1}$$
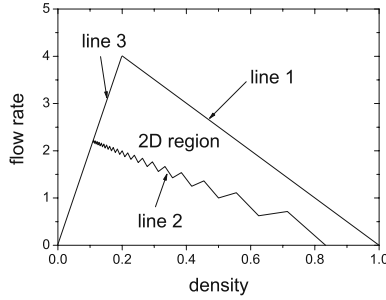
Fig. 1. The steady states of the model, which cover a two-dimensional region in the flow-density plane in the noiseless limit (i.e., $p_d = 0$). Line 1 is determined by $v = d$, line 2 is determined by $v = \min(v')$ and v' is determined by $v' = \lfloor \frac{-T + \sqrt{T^2 + \frac{2}{D}\left(d + \frac{v'^2}{2D}\right)}}{1/D} \rfloor$, line 3 is determined by $v = v_{\max}$. Here v is velocity and d is spatial gap of the steady state. The parameters $T = 1, D = 1, v_{\max} = 20$. Each cell is 1.5 m and one vehicle occupies five cells.

Here $\frac{v'^2}{2D} + v'T$ is braking distance of a car travelling with velocity v' and $\frac{v_{n-1}^2(t)}{2D}$ is braking distance of the car $n-1$. Note that T is not necessarily to be one and D is not necessarily to be an integer in the model. It is obvious that when D is extremely large and $T \leq 1$, the model reduces to NaSch model.

In our model, the vehicles brake with comfortable deceleration if possible. However, if the comfortable deceleration could not guarantee safety (i.e., Eq. (1) is not met), the vehicles will brake with much larger deceleration.

In the noiseless limit, the steady states of the model cover a two-dimensional region as shown in Fig. 1. Therefore, the model is within the framework of Kerner's three-phase traffic theory [1].

3   Approximation Solution

Fig. 2 shows fundamental diagram of the model with parameters $D = 1$, $T = 1$, $p_d = 0.1$. A critical density ρ_c is identified. When $\rho < \rho_c$, free flow exists. When $\rho > \rho_c$, homogeneous congested flow is identified (see Fig. 3). It can be seen that the velocities of the vehicles fluctuate around 12 and 13. Velocities smaller than 10 or larger than 14 are seldom observed. Due to homogeneity of the congested flow, the finite size effect is trivial (Fig. 2).

Based on this fact, if we could obtain approximation solution of small sized traffic system with two vehicles, then the solution can also be regarded as approximation solution of large system.

Now we investigate such a small system with two vehicles by using car-oriented mean-field theory [13]. Let us consider a specific density $\rho = 1/6$, which corresponds to system size $L = 60$. Since the traffic flow is quite homogeneous, we
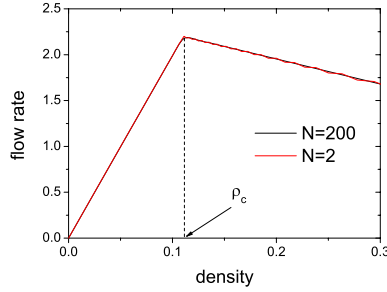
Fig. 2. Fundamental diagram of the model with parameters $D = 1$, $T = 1$, $p_d = 0.1$. The system size $L = N(d + l)$, N is the number of vehicles, d is average spatial gap of vehicles. The flow rate of system consisting of two vehicles ($N = 2$) is almost identical to that of large system.
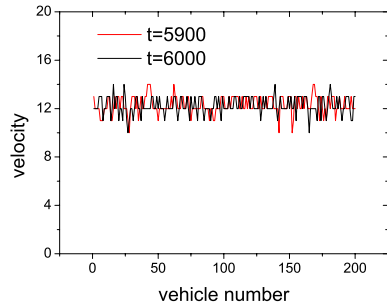

Fig. 3. Snapshots of velocities of the vehicles in congested flow. The density $\rho = 1/6$, i.e., $d = 25$.

only consider the following configurations of the two vehicles and assume the appearance probabilities of other configurations could be neglected [1]:

$$12-11-26, 13-12-25, 12-12-25, 12-11-25, 12-10-25, 11-11-25, 13-12-24,$$

$$13-11-24, 12-12-24, 12-11-24, 11-11-24, 13-11-23, 12-11-23, 11-11-23.$$

Here the first number denotes the velocity of one vehicle, the third number denotes the spatial gap in front of the vehicle, and the second number denotes the velocity of the other vehicles. Note due to the symmetry, $x - y - z$ and $y - x - (L - z)$ denote the same configuration.

We study the evolution of the configurations. For example, consider configuration 11-11-25. Without considering randomization, this configuration will evolve into 12-12-25. When considering randomization, 12-12-25 will turn into 11-11-25 with probability p_d^2 (both vehicles are randomized), 12-11-24 with probability

---

[1] Generally speaking, considering more configurations will lead to more accurate approximation solution.

Table 1. The table shows other equations obtained from mean field approximation

From	we have
$\frac{dP_{13-12-25}}{dt} = 0$	$(P_{12-12-24} + P_{13-12-24})(1 - p_d)^2 \approx P_{13-12-25}$
$\frac{dP_{12-12-25}}{dt} = 0$	$(P_{11-11-25} + P_{12-11-25})(1 - p_d)^2 + P_{13-12-25}(1 - p_d)p_d \approx P_{12-12-25}(1 - (1 - p_d)^2)$
$\frac{dP_{12-11-25}}{dt} = 0$	$(P_{12-12-24} + P_{13-12-24})p_d^2 + (P_{12-11-26} + P_{11-11-24} + P_{12-11-24} + P_{13-11-24})(1 - p_d)p_d$ $\approx P_{12-11-25}$
$\frac{dP_{12-10-25}}{dt} = 0$	$(P_{11-11-23} + P_{12-11-23} + P_{13-11-23})(1 - p_d)p_d \approx P_{12-10-25}$
$\frac{dP_{11-11-25}}{dt} = 0$	$(P_{12-12-25} + P_{12-11-25})p_d^2 + P_{12-10-25}(1 - p_d)^2 \approx P_{11-11-25}(1 - p_d^2)$
$\frac{dP_{13-12-24}}{dt} = 0$	$P_{13-12-25}(1 - p_d)^2 \approx P_{13-12-24}$
$\frac{dP_{13-11-24}}{dt} = 0$	$(P_{12-12-24} + P_{13-12-24})(1 - p_d)p_d \approx P_{13-11-24}$
$\frac{dP_{12-12-24}}{dt} = 0$	$P_{13-12-24}(1 - p_d)p_d + (P_{12-11-26} + P_{11-11-24} + P_{13-11-24})(1 - p_d)^2$ $\approx P_{12-12-24}(1 - (1 - p_d)p_d)$
$\frac{dP_{12-11-24}}{dt} = 0$	$(P_{11-11-25} + P_{12-12-25} + P_{12-11-25})2(1 - p_d)p_d + P_{13-12-25}p_d^2 \approx P_{12-11-24}$
$\frac{dP_{11-11-24}}{dt} = 0$	$(P_{12-11-26} + P_{12-11-24} + P_{13-11-24})p_d^2 \approx P_{11-11-24}(1 - p_d^2)$
$\frac{dP_{13-11-23}}{dt} = 0$	$P_{13-12-25}(1 - p_d)p_d \approx P_{13-11-23}$
$\frac{dP_{12-11-23}}{dt} = 0$	$(P_{12-11-26} + P_{11-11-24} + P_{12-11-24} + P_{13-11-24})(1 - p_d)p_d \approx P_{12-11-23}$

$2(1 - p_d)p_d$ (one vehicle is randomized and the other is not) and remains 12-12-25 with probability $(1 - p_d)^2$ (neither vehicles are randomized). This means the configuration

$$11 - 11 - 25 \rightarrow \begin{cases} 12 - 12 - 25 & \text{with probability } (1 - p_d)^2 \\ 11 - 11 - 25 & \text{with probability } p_d^2 \\ 12 - 11 - 24 & \text{with probability } 2(1 - p_d)p_d \end{cases}$$

The evolution of other configurations could be obtained similarly.

Based on these, the master equation of the evolution of the configurations could be written out. The master equation of configuration 12-11-26 is

$$\frac{dP_{12-11-26}}{dt} \approx (P_{11-11-23} + P_{12-11-23} + P_{13-11-23})(1 - p_d)^2 - P_{12-11-26}. \quad (2)$$

Here " $\approx$ " is used because we have neglected many possible configurations, whose appearance probabilities are very small. In the steady state, $\frac{dP_{12-11-26}}{dt} = 0$. Thus, we have

$$(P_{11-11-23} + P_{12-11-23} + P_{13-11-23})(1 - p_d)^2 \approx P_{12-11-26}. \quad (3)$$

Similarly, other equations could be obtained as shown in Table 1.

Finally, our assumption gives

$$P_{12-11-26} + P_{13-12-25} + P_{12-12-25} + P_{12-11-25} + P_{12-10-25} + P_{11-11-25} + P_{13-12-24}$$
$$P_{13-11-24} + P_{12-12-24} + P_{12-11-24} + P_{11-11-24} + P_{13-11-23} + P_{12-11-23} + P_{11-11-23} \approx 1$$
$$(4)$$

Now we have 14 variables and 14 linear equations [2]. The equations could be solved. The average velocity of the vehicles is then calculated by

---

[2] Note from $\frac{dP_{11-11-23}}{dt} = 0$, we can obtain another equation. However, this is not an independent equation.

$$\begin{aligned}
\bar{v} = {} & 11.5P_{12-11-26} + 12.5P_{13-12-25} + 12P_{12-12-25} + 11.5P_{12-11-25} \\
& + 11P_{12-10-25} + 11P_{11-11-25} + 12.5P_{13-12-24} + 12P_{13-11-24} \\
& + 12P_{12-12-24} + 11.5P_{12-11-24} + 11P_{11-11-24} + 12P_{13-11-23} \\
& + 11.5P_{12-11-23} + 11P_{11-11-23}
\end{aligned} \tag{5}$$

and the result is $\bar{v} = 12.188$, which is in very good agreement with simulation result $\bar{v} = 12.19$.

If the density is changed, then one needs to study the master equations of different configurations. It can be verified that the approximation solution is always in good agreement with simulation result at any density.

4   Discussion

In this section, we discuss the possible relationship between homogeneous congested flow and the synchronized flow. To this end, we firstly study the synchronized flow in three CA models, i.e., the model proposed by Lee et al. (model A) [14], the Kerner-Klenov-Wolf model (model B) [15], and the model proposed by Jiang and Wu (Model C) [16].

Fig. 4(a) shows the fundamental diagram of model A. Two critical densities ρ_{c1} and ρ_{c2} are identified. When $\rho < \rho_{c1}$, the traffic is in free flow. When $\rho_{c1} < \rho < \rho_{c2}$, synchronized flow appears in free flow. Fig. 5(a) shows the typical snapshot of velocities corresponding to the coexistence phenomenon. With the increase of density, more and more vehicles are involved in the synchronized flow state (Fig. 5(b)). When $\rho > \rho_{c2}$, the free flow disappears and all vehicles are in synchronized flow state (Fig. 5(c)). With the further increase of density, the average velocity of the synchronized flow decreases (Fig. 5(d)).

Fig. 4(b) shows the fundamental diagram of model B. When ρ is smaller than ρ_c, which corresponds to maximum flow rate, light synchronized flow has already appeared (Fig. 6(a)). With the increase of density, the coexistence of light synchronized flow and heavy synchronized flow is identified (Fig. 6(b)). With the further increase of density, the average velocity of synchronized flow
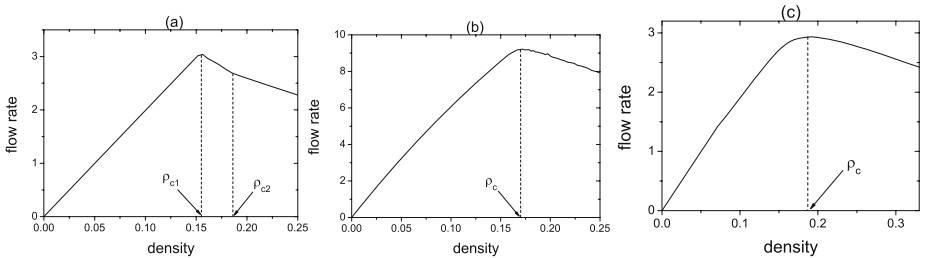

Fig. 4. Fundamental diagram of (a) model A, (b) model B, (c) model C. In (a), the parameters are the same as in Ref.[13]. In (b), $p_{a1} = p_{a2} = 0.052$, other parameters are the same as in parameter set I in Ref.[14]. In (c), $h = 3$, other parameters are the same as in Ref.[15]. Note that in model B, each cell is 0.5 m and one vehicle occupied 15 cells.
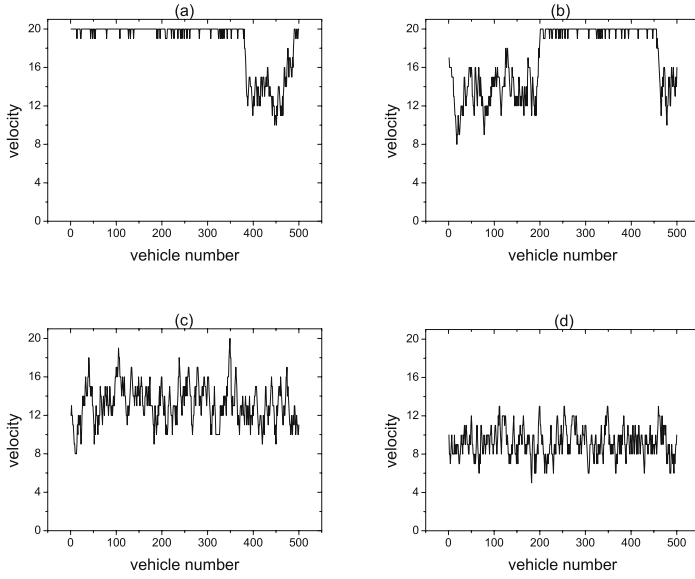
Fig. 5. Snapshots of velocities in model A. (a) $\rho = 0.1613$, (b) $\rho = 0.1724$, (c) $\rho = 0.2$, (d) $\rho = 0.25$.
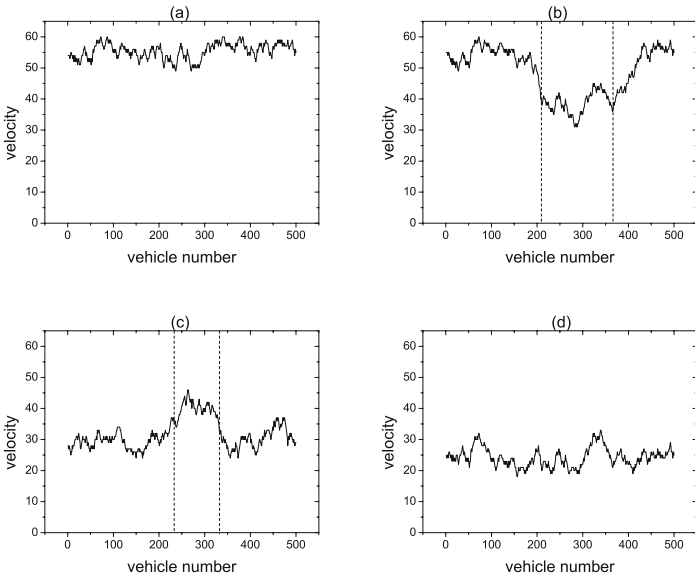

Fig. 6. Snapshots of velocities in model B. (a) $\rho = 0.1667$, (b) $\rho = 0.1875$, (c) $\rho = 0.25$, (d) $\rho = 0.3$. In (b) and (c), the dashed lines show the boundaries of the coexisting states.
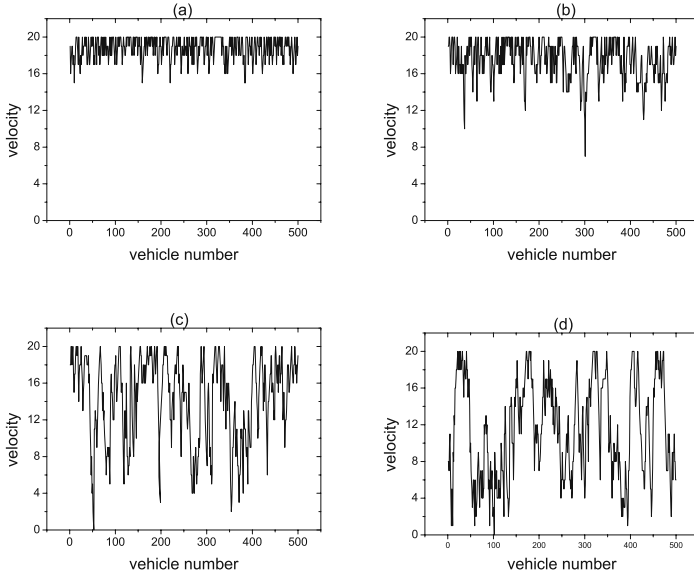
Fig. 7. Snapshots of velocities in model C. (a) $\rho = 0.125$, (b) $\rho = 0.1667$, (c) $\rho = 0.2$, (d) $\rho = 0.25$.
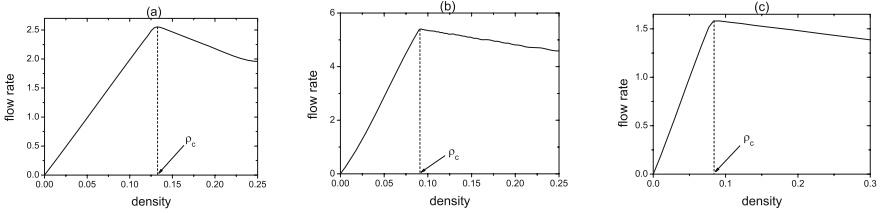

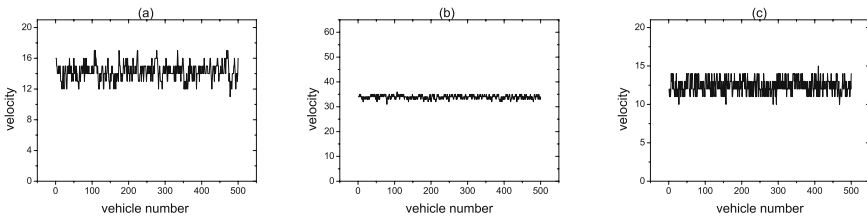**Fig. 8.** Fundamental diagram of slightly modified (a) model A, (b) model B, (c) model C

Fig. 9. Snapshots of velocities in (a) modified model A, $\rho = 0.1667$, (b) modified model B, $\rho = 0.15$, (c) modified model C, $\rho = 0.125$

decreases, but the coexistence phenomenon is still observed (Fig. 6(c)). When the density is large, the coexistence phenomenon gradually disappears (Fig. 6(d)).

Fig. 4(c) shows the fundamental diagram of model C. The transition from free flow to synchronized flow is smooth. Fig. 7 shows typical snapshots of velocities at different densities. One can see that the fluctuations are much stronger than in models A and B.

Although the synchronized flows exhibit different features in the three models, they are all closely related to homogeneous congested flow. Fig. 8(a) shows the fundamental diagram of model A, in which it is assumed that the drivers are always in defensive state ($\gamma = 1$). Fig. 8(b) shows the fundamental diagram of model B, in which the acceleration noise is set to zero, i.e., $p_{a1} = p_{a2} = 0$. Fig. 8(c) shows the fundamental diagram of model C, in which the brake lights are always set to be on ($b_n = 1$). One can see that the three fundamental diagrams are similar to that in Fig. 2. When $\rho < \rho_c$, the traffic is in free flow. When $\rho > \rho_c$, the traffic becomes homogeneous congested flow (Fig. 9).

Our results thus demonstrate that homogeneous congested flow might be backbone of synchronized flow. By including different mechanisms into the homogeneous congested flow, synchronized flow with different features could be reproduced. Presently we do not know which mechanism is real origin of synchronized flow, which needs to be further investigated.

5   Conclusion

To summarize, we have proposed a CA traffic flow model, in which the finite size effect is trivial because the congested flow is quite homogeneous. As a result, the approximation solution of a small sized system can be regarded as solution of large system. We have investigated the approximation solution of a small traffic system with two vehicles. The analytical result is in good agreement with simulation.

We also discussed the relationship between homogeneous congested flow and synchronized flow. It is demonstrated that the synchronized flow is closely related with homogeneous congested flow. By introducing different mechanisms into the homogeneous congested flow, synchronized flow with different features could be reproduced.

Acknowledgments

References

1. Kerner, B.S.: The Physics of Traffic. Springer, New York (2004)
2. Chowdhury, D., Santen, L., Schadschneider, A.: Statistical physics of vehicular traffic and some related systems. Phys. Rep. 329, 199–329 (2000)

3. Helbing, D.: Traffic and related self-driven many-particle systems. Rev. Mod. Phys. 73, 1067–1141 (2001)
4. Nagatani, T.: The physics of traffic jams. Rep. Prog. Phys. 65, 1331–1386 (2002)
5. Nagel, K., Wagner, P., Woesler, R.: Still flowing: Approaches to traffic flow and traffic jam modeling. Oper. Res. 51, 681–710 (2003)
6. Maerivoet, S., De Moor, B.: Cellular automata models of road traffic. Phys. Rep. 419, 1–64 (2005)
7. Nagel, K., Schreckenberg, M.: A cellular automaton model for freeway traffic. J. Physique I 2, 2221–2229 (1992)
8. Kerner, B.S., Rehborn, H.: Experimental properties of phase transitions in traffic flow. Phys. Rev. Lett. 79, 4030–4033 (1997)
9. Kerner, B.S., Rehborn, H.: Experimental features and characteristics of traffic jams. Phys. Rev. E 53, R1297–R1300 (1996)
10. Kerner, B.S., Rehborn, H.: Experimental properties of complexity in traffic flow. Phys. Rev. E 53, R4275–R4278 (1996)
11. Kerner, B.S.: Experimental features of self-organization in traffic flow. Phys. Rev. Lett. 81, 3797–3800 (1998)
12. Kerner, B.S.: Empirical macroscopic features of spatial-temporal traffic patterns at highway bottlenecks. Phys. Rev. E 65, 046138 (2002)
13. Schadschneider, A., Schreckenberg, M.: Car-oriented mean-field theory for traffic flow models. J. Phys. A 30, L69–L75 (1997)
14. Lee, H.K., Barlovic, R., Schreckenberg, M., Kim, D.: Mechanical restriction versus human overreaction triggering congested traffic states. Phys. Rev. Lett. 92, 238702 (2004)
15. Kerner, B.S., Klenov, S.L., Wolf, D.E.: Cellular automata approach to three-phase traffic theory. J. Phys. A 35, 9971–10013 (2002)
16. Jiang, R., Wu, Q.S.: Cellular automata models for synchronized traffic flow. J. Phys. A 36, 381–390 (2003)